Journal of Solid State Chemistry **152,** 174–182 (2000)
doi:10.1006/jssc.2000.8680, available online at http://www.idealibrary.com on IDEAL®

Two- and Three-Dimensional Mixed-Valence Cu(I)–Cu(II) Coordination Polymers: Syntheses and Characterization of α-, β-$[Cu_2X(C_5H_3N_2O_2)_2(H_2O)]$ (X = Cl, Br)

Li-Min Zheng,[1] Xiqu Wang, and Allan J. Jacobson[2]

Department of Chemistry, University of Houston, Houston, Texas 77204-5641

Novel mixed valence compounds with the formula α-$[Cu_2X(C_5H_3N_2O_2)_2(H_2O)]_n$ [X = Cl(1), Br(3), $C_5H_3N_2O_2$ = 2-pyrazinecarboxylate] and their isomers β-$[Cu_2X(C_5H_3N_2O_2)_2(H_2O)]_n$ [X = Cl(2), Br(4)] have been synthesized and structurally characterized. Crystal data: 1, orthorhombic, *Pbca*, a = 12.8040(7), b = 7.7323(4), c = 26.104(1) Å, V = 2584.4(2) Å^3, Z = 8, $R1$ = 0.0559; 2, triclinic, $P\bar{1}$, a = 6.1908(7), b = 7.7246(8), c = 13.968(2) Å, α = 78.853(2), β = 81.455(2), γ = 78.036(2)°, V = 637.0(1) Å^3, Z = 2, $R1$ = 0.0592; 3, orthorhombic, *Pbca*, a = 12.7082(6), b = 7.7676(4), c = 26.1548(12) Å, V = 2581.8(2) Å^3, Z = 8, $R1$ = 0.0257; 4, triclinic, $P\bar{1}$, a = 6.2462(5), b = 7.7568(6), c = 14.1121(10) Å, α = 78.082(1), β = 81.702(1), γ = 79.096(1)°, V = 652.97(9) Å^3, Z = 2, $R1$ = 0.0290. The α-isomers 1 and 3 have two-dimensional layer structures which are composed of mixed valence chains of $[Cu^ICu^{II}(C_5H_3N_2O_2)_2(H_2O)]$ and chains of corner-sharing $\{Cu^IN_2X_2\}$ tetrahedra. The β-isomers 2 and 4, however, have three-dimensional structures with the $[Cu^ICu^{II}(C_5H_3N_2O_2)_2]$ chains interconnected by an alternative arrangement of $\{Cu^{II}N_2O_4\}$ octahedra, $\{Cu^IN_2OX\}$ tetrahedra and $\{Cu^{II}N_2O_2X_2\}$ octahedra. The spectroscopic and magnetic properties have been investigated. © 2000 Academic Press

Key Words: **pyrazine carboxylate; copper; mixed valence; coordination polymer.**

INTRODUCTION

Studies on the mixed-valence Cu(I)/Cu(II) complexes are of intense interest both in biochemistry and in inorganic chemistry (1–3). Such complexes may serve as possible models for copper proteins or provide valuable information on electron-transfer mechanisms. Examples of Cu(I)/Cu(II) complexes can be summarized into three classes, based on the coordination geometry of the Cu(I) and Cu(II) ions (4). When the Cu(I) and Cu(II) ions have the same or nearly identical coordination geometries (Class II or III), significant *d–d* interactions between Cu(I) and Cu(II) are expected. The *d–d* interaction, however, has also been observed in a few compounds where the Cu(I) and Cu(II) have the distinctly different geometries typical for each oxidation state (Class I) (5).

Pyrazine has been frequently studied in the course of electron-transfer research (6). Mixed valence copper compounds containing the pyrazine bridging ligand are surprisingly rare (we have found no structure data on such compounds in the Cambridge Structure Database). The 2-pyrazinecarboxylic acid (abbreviated as 2-pzcH), like pyrazine, is also capable of linking metal ions into polymeric compounds. The additional carboxylate group, together with its neighboring N atom from the pyrazine group, is expected to favor a stable five-member ring with Cu(II) ions and, hence, generate different coordination environments for the two metal ions connected through the bridge. Such a coordination variability allows for the design and synthesis of novel mixed valence copper(I/II) compounds. In this paper, we describe the hydrothermal syntheses and characterizations of four new mixed-valence copper compounds including α-, β-$[Cu_2X(C_5H_3N_2O_2)_2(H_2O)]_n$ (X = Cl, Br) with two- and three-dimensional structures. It is worth noting that, as far as we are aware, only one copper polymer $[KCu_2(2\text{-pzc})(N_3)_4]_n$ which contains 2-pzc bridging ligand has been structurally characterized (7).

EXPERIMENTAL

Materials and Methods

All the starting materials were reagent grade and used as purchased. The infrared spectra were recorded on a Galaxy FTIR 5000 series spectrometer with pressed KBr pellets. Thermal analyses were performed in air with a heating rate of 5°C/min on a TGA V5.1A Dupont 2100 instrument. The

[1] On leave from State Key Laboratory of Coordination Chemistry, Coordination Chemistry Institute, Nanjing University, Nanjing 210093, P.R. China.

[2] To whom correspondence should be addressed. E-mail: ajjacob@uh.edu.

0022-4596/00 $35.00

UV–vis diffuse reflectance spectra were measured on a Cary 500 UV–vis spectrophotometer. Magnetic susceptibility data were obtained on polycrystalline samples from 2 to 300 K in a magnetic field of 5 kG using a SQUID magnetometer.

Syntheses of α-$[Cu_2Cl(C_5H_3N_2O_2)_2(H_2O)]_n$ (**1**) *and* β-$[Cu_2Cl(C_5H_3N_2O_2)_2(H_2O)]_n$ (**2**)

The compounds were initially prepared by heating a mixture of $CuCl_2 \cdot 2H_2O$ (0.0857 g, 0.5 mmol), 2-pyrazinecarboxylic acid (0.0636 g, 0.5 mmol), and H_2O (8 mL) in a Teflon-lined autoclave (23 mL) at 160°C for 23 h. After slow cooling, black prismatic crystals of **1** appeared as a minor phase, together with a few dark red plate-like crystals of **2** and a large amount of unidentified orange thin plates and red needle-like crystals. The red needles were identified as the known compound $[CuCl(pz)]_n$ (8, 9). A single phase of **1** can be obtained by hydrothermal treatment of a mixture of $CuCl_2 \cdot 2H_2O$ (0.0854 g, 0.5 mmol), 2-pyrazinecarboxylic acid (0.0621 g, 0.5 mmol), and H_2O (8 mL) at 140°C for 45 h, as judged by the powder X-ray diffraction pattern (yield ca. 62%). IR (KBr) for **1**: 3341m (br), 3065w, 1678s, 1597m, 1522w, 1468m, 1414m, 1329s, 1283m, 1177m, 1157m, 1062m, 1051m, 870m, 793m, 743m, 721w, 488m, 476m cm^{-1}.

The preparation of **2** was also optimized. A major phase of **2** was obtained by reacting $CuCl_2 \cdot 2H_2O$ (0.3418 g, 2.0 mmol), 2-pyrazinecarboxylic acid (0.2489 g, 2.0 mmol), and H_2O (8 mL) at 140°C for 29 h, together with the unidentified brown crystalline impurities. The dark red crystals of **2** were manually collected with the purity confirmed by the powder X-ray diffraction pattern (yield ca. 68%). IR (KBr) for **2**: 3316m, 3059w, 1661s, 1645s, 1595m, 1526w, 1478w, 1462w, 1416m, 1366s, 1358s, 1283w, 1177m, 1163m, 1154m, 1059m, 1049m, 870m, 841w, 793m, 743m, 677w, 598w, 557w, 474m cm^{-1}.

Syntheses of α-$[Cu_2Br(C_5H_3N_2O_2)_2(H_2O)]_n$ (**3**) *and* β-$[Cu_2Br(C_5H_3N_2O_2)_2(H_2O)]_n$ (**4**)

Compound **3** was first obtained as a major phase by hydrothermal reaction of $CuSO_4 \cdot 5H_2O$ (0.2493 g, 1.0 mmol), KBr (0.0608 g, 0.5 mmol), 2-pyrazinecarboxylic acid (0.1241 g, 1.0 mmol), and H_2O (8 mL) at 160°C for 20 h, together with small amount of yellow crystals and a few dark red plate-like crystals of **4**. The measured cell constants of the yellow crystals (10) revealed that its structure is closely related to the known compound $[Cu_2Cl_2(pz)]_n$ (11). A single phase of **3** was, afterward, obtained through the reaction of $CuSO_4 \cdot 5H_2O$ (0.2506 g, 1.0 mmol), KBr (0.1245 g, 1.0 mmol), 2-pyrazinecarboxylic acid (0.1207 g, 1.0 mmol), and H_2O (8 mL) at 140°C for 29 h (yield ca. 68%). IR (KBr) for **3**: 3360m (br), 3069w, 1676s, 1597m, 1520w, 1468m, 1416m, 1335s, 1283m, 1169m, 1159m, 1063m, 1053m, 868m, 795m, 743m, 721w, 490m, 473m cm^{-1}.

The hydrothermal reaction of a mixture of $CuSO_4 \cdot 5H_2O$ (0.4999 g, 2.0 mmol), KBr (0.3586 g, 3.0 mmol), 2-pyrazinecarboxylic acid (0.2496 g, 2.0 mmol), and H_2O (8 mL) at 140°C for 16 h resulted in the formation of **4** as a major phase together with the compound **3**. IR (KBr) for **4**: 3291m, 3057m, 1657s, 1645s, 1595m, 1526w, 1478w, 1464w, 1425m, 1416m, 1366s, 1358s, 1283w, 1177m, 1157m, 1061m, 1049m, 868m, 842w, 793m, 743m, 719w, 677w, 611w, 557w, 475m cm^{-1}.

X-Ray Crystallographic Analysis

Single crystal X-ray data were measured on a SMART platform diffractometer equipped with a 1K CCD area detector using graphite-monochromatized Mo$K\alpha$ radiation at 223 K for **1–4**. For each phase a hemisphere of data (1271 frames at 5 cm detector distance) was collected using a narrow-frame method with scan widths of 0.30° in ω and an exposure time of 30 s/frame. The first 50 frames were remeasured at the end of data collection to monitor instrument and crystal stability, and the maximum correction applied on the intensities was $< 1\%$. The data were integrated using the Siemens SAINT program (12), with the intensities corrected for Lorentz factor, polarization, air absorption, and absorption due to variation in the path length through the detector faceplate. Absorption corrections were made using the program SADABS (13). The structures were solved by direct methods and refined using SHELXTL (14). All nonhydrogen positions were derived by direct methods and refined anisotropically in the final refinements. The hydrogen atoms were located from difference maps and refined isotropically with isotropic thermal parameters or distance constraints. Crystallographic and refinement details are summarized in Table 1. Atomic coordinates for **1–4** are listed in Tables 2–5, and selected bond lengths and angles in Tables 6–9.

RESULTS AND DISCUSSION

Syntheses and Preliminary Characterization

Under suitable hydrothermal reaction conditions, four new compounds **1–4** have been successfully synthesized containing mixed valence copper(I/II) ions. We have found that in similar reactions higher temperatures (160°C or above) and/or longer reaction times promote the formation of cuprous compounds $[CuX(pz)]_n$ and/or $[Cu_2X_2(pz)]_n$ (pz = pyrazine), with the decarboxylation of 2-pyrazinecarboxylate. The production of Cu(I) in these compounds from CuX_2 is presumably caused by the decarboxylation reaction of 2-pyrazinecarboxylic acid in the presence of halide anions. The rate differences of such decarboxylation at

TABLE 1
Crystal Data for 1–4

Compound	**1**	**2**	**3**	**4**
Empirical formula	$C_{10}H_8ClCu_2N_4O_5$	$C_{10}H_8ClCu_2N_4O_5$	$C_{10}H_8BrCu_2N_4O_5$	$C_{10}H_8BrCu_2N_4O_5$
Formula weight	426.73	426.73	471.19	471.19
Temperature (K)	223	223	223	223
Crystal system	Orthorhombic	Triclinic	Orthorhombic	Triclinic
Space group	*Pbca*	$P\bar{1}$	*Pbca*	$P\bar{1}$
a (Å)	12.8040(7)	6.1908(7)	12.7082(6)	6.2462(5)
b (Å)	7.7323(4)	7.7246(8)	7.7676(4)	7.7568(6)
c (Å)	26.1040(10)	13.968(2)	26.1548(12)	14.1121(10)
α (°)		78.853(2)		78.082(1)
β (°)		81.455(2)		81.702(1)
γ (°)		78.036(2)		79.096(1)
Volume (Å^3), Z	2584.4(2), 8	637.0(1), 2	2581.8(2), 8	652.97(9), 2
Crystal size (mm)	$0.35 \times 0.08 \times 0.07$	$0.08 \times 0.05 \times 0.03$	$0.28 \times 0.12 \times 0.10$	$0.25 \times 0.12 \times 0.06$
D_c (g cm^{-3})	2.193	2.225	2.424	2.397
μ (cm^{-1})	35.29	35.79	64.21	63.47
Independent reflections	3082 [$R_{int} = 0.0499$]	2657 [$R_{int} = 0.0344$]	3117 [$R_{int} = 0.0264$]	2843 [$R_{int} = 0.0195$]
Number of parameters	223	228	232	235
Goodness-of-fit on F^2	1.175	1.072	1.111	1.056
$R1$, $wR2$ [$I > 2\sigma(I)$][a] (all data)	0.0559, 0.1314	0.0592, 0.1118	0.0257, 0.0544	0.0290, 0.0748
	0.0758, 0.1466	0.0968, 0.1277	0.0353, 0.0574	0.0331, 0.0860
Extinction coefficient		0.00051(5)	0.016(2)	
$\Delta\rho_{max}$, $\Delta\rho_{min}$ (e Å^{-3})	1.592, −0.628	0.744, −0.808	0.772, −0.430	0.719, −0.766

[a] $R_1 = \sum||F_o| - |F_c||/\sum|F_o|$. $wR_2 = [\sum w(F_o^2 - F_c^2)^2/\sum w(F_o^2)^2]^{1/2}$.

different temperatures might have directed the formation of the α- and β-phases.

The IR spectra of **1–4** exhibit several bands around 3300 cm^{-1}, corresponding to the O–H stretching of coordinated water molecules. The peaks that appeared at 1650–1680 cm^{-1} [ν(C=O)] and 1330–1360 cm^{-1} [ν(C–O)] indicate a monodentate coordination of the carboxylic group to the metal atoms. The vibration bands at ca. 1051,

TABLE 2
Atomic Coordinates and Equivalent Isotropic Displacement Parameters (Å^3) for 1

Atom	x	y	z	U(eq)[a]
Cu(1)	0.6102(1)	0.2593(1)	0.6825(1)	0.014(1)
Cu(2)	0.6687(1)	0.0875(1)	0.4347(1)	0.022(1)
Cl(1)	0.8238(1)	0.2562(2)	0.4360(1)	0.025(1)
O(1)	0.5931(3)	0.4857(4)	0.6513(1)	0.019(1)
O(2)	0.5742(5)	0.6173(5)	0.5754(2)	0.045(1)
O(3)	0.6050(3)	0.0295(4)	0.7136(1)	0.018(1)
O(4)	0.6159(3)	−0.1075(5)	0.7888(2)	0.028(1)
O(1W)	0.7822(3)	0.2579(5)	0.6767(2)	0.026(1)
N(1)	0.5942(3)	0.1776(5)	0.6101(2)	0.016(1)
N(2)	0.6157(3)	0.1269(5)	0.5053(2)	0.018(1)
N(3)	0.6167(3)	0.3364(5)	0.7556(2)	0.014(1)
N(4)	0.6324(3)	0.3832(5)	0.8613(2)	0.016(1)
C(1)	0.5993(4)	0.0190(6)	0.5906(2)	0.019(1)
C(2)	0.6102(4)	−0.0067(6)	0.5386(2)	0.020(1)
C(3)	0.6060(4)	0.2869(6)	0.5253(2)	0.020(1)
C(4)	0.5947(4)	0.3117(6)	0.5769(2)	0.017(1)
C(5)	0.5865(4)	0.4876(6)	0.6020(2)	0.022(1)
C(6)	0.6245(4)	0.4942(6)	0.7760(2)	0.017(1)
C(7)	0.6312(4)	0.5177(7)	0.8286(2)	0.018(1)
C(8)	0.6256(4)	0.2236(6)	0.8410(2)	0.017(1)
C(9)	0.6178(4)	0.2000(6)	0.7885(2)	0.015(1)
C(10)	0.6120(4)	0.0245(6)	0.7632(2)	0.016(1)

[a] U(eq) is defined as one-third of the trace of the orthogonalized U_{ij} tensor.

TABLE 3
Atomic Coordinates and Equivalent Isotropic Displacement Parameters (Å^2) for 2

Atom	x	y	z	U(eq)[a]
Cu(1)	0.0000	0.0000	1.0000	0.016(1)
Cu(2)	0.1802(1)	0.7812(1)	0.7248(1)	0.021(1)
Cu(3)	−0.5000	1.5000	0.5000	0.019(1)
Cl	0.5197(3)	0.7463(2)	0.6277(1)	0.021(1)
O(1)	0.2451(7)	0.0590(5)	1.0544(3)	0.017(1)
O(2)	0.4245(8)	0.2876(6)	1.0452(3)	0.024(1)
O(3)	−0.6905(7)	1.3963(6)	0.6086(3)	0.017(1)
O(4)	−0.6724(8)	1.2082(6)	0.7505(3)	0.029(1)
O(1W)	0.2423(8)	0.8987(6)	0.8575(3)	0.020(1)
N(1)	−0.0201(8)	0.2530(7)	0.9239(4)	0.015(1)
N(2)	0.0743(9)	0.5714(7)	0.8120(4)	0.018(1)
N(3)	−0.2614(8)	1.3088(6)	0.5568(4)	0.014(1)
N(4)	−0.0043(8)	1.0077(7)	0.6560(4)	0.015(1)
C(1)	−0.1457(11)	0.3421(9)	0.8546(5)	0.017(1)
C(2)	−0.0957(11)	0.4997(8)	0.7977(5)	0.019(1)
C(3)	0.1928(10)	0.4821(8)	0.8867(5)	0.014(1)
C(4)	0.1487(9)	0.3225(7)	0.9406(4)	0.011(1)
C(5)	0.2849(10)	0.2153(8)	1.0199(4)	0.014(1)
C(6)	−0.0498(11)	1.2565(8)	0.5243(5)	0.016(1)
C(7)	0.0789(11)	1.1033(8)	0.5739(5)	0.018(1)
C(8)	−0.2167(10)	1.0635(8)	0.6889(5)	0.015(1)
C(9)	−0.3458(10)	1.2136(8)	0.6399(4)	0.014(1)
C(10)	−0.5874(11)	1.2756(8)	0.6705(5)	0.016(1)

[a] U(eq) is defined as one-third of the trace of the orthogonalized U_{ij} tensor.

TABLE 4
Atomic Coordinates and Equivalent Isotropic Displacement Parameters (Å²) for 3

Atom	*x*	*y*	*z*	*U*(eq)[a]
Cu(1)	0.6008(1)	0.2461(1)	0.1224(1)	0.016(1)
Cu(2)	0.6710(1)	0.0693(1)	0.3727(1)	0.021(1)
Br	0.8524(1)	0.2161(1)	0.3730(1)	0.020(1)
N(1)	0.6052(2)	0.1633(3)	0.1952(1)	0.014(1)
N(2)	0.6352(2)	0.1085(3)	0.2996(1)	0.015(1)
N(3)	0.6087(2)	0.3304(3)	0.0500(1)	0.014(1)
N(4)	0.6342(2)	0.3872(3)	− 0.0542(1)	0.016(1)
O(1)	0.5993(2)	0.4719(2)	0.1549(1)	0.019(1)
O(2)	0.6260(2)	0.6001(2)	0.2302(1)	0.026(1)
O(3)	0.5974(2)	0.0215(2)	0.0895(1)	0.019(1)
O(4)	0.6142(2)	− 0.1057(2)	0.0133(1)	0.027(1)
O(1W)	0.7819(2)	0.2493(3)	0.1231(1)	0.028(1)
C(1)	0.6075(2)	0.0045(3)	0.2145(1)	0.017(1)
C(2)	0.6230(2)	− 0.0219(3)	0.2665(1)	0.016(1)
C(3)	0.6321(2)	0.2690(3)	0.2797(1)	0.016(1)
C(4)	0.6173(2)	0.2959(3)	0.2277(1)	0.015(1)
C(5)	0.6143(2)	0.4726(3)	0.2035(1)	0.016(1)
C(6)	0.6184(2)	0.4901(3)	0.0315(1)	0.015(1)
C(7)	0.6309(2)	0.5176(3)	− 0.0206(1)	0.016(1)
C(8)	0.6255(2)	0.2271(3)	− 0.0351(1)	0.017(1)
C(9)	0.6134(2)	0.1989(3)	0.0168(1)	0.014(1)
C(10)	0.6074(2)	0.0215(3)	0.0404(1)	0.016(1)

[a] *U*(eq) is defined as one-third of the trace of the orthogonalized U_{ij} tensor.

TABLE 5
Atomic Coordinates and Equivalent Isotropic Displacement Parameters (Å²) for 4

Atom	*x*	*y*	*z*	*U*(eq)[a]
Cu(1)	0.0000	0.0000	1.0000	0.014(1)
Cu(2)	0.1652(1)	0.7972(1)	0.7331(1)	0.019(1)
Cu(3)	− 0.5000	1.5000	0.5000	0.018(1)
Br	0.5199(1)	0.7579(1)	0.6306(1)	0.019(1)
O(1)	0.2443(4)	0.0581(3)	1.0545(2)	0.017(1)
O(2)	0.4310(4)	0.2833(3)	1.0445(2)	0.023(1)
O(3)	− 0.6899(4)	1.3973(3)	0.6096(2)	0.018(1)
O(4)	− 0.6714(4)	1.2202(3)	0.7553(2)	0.027(1)
O(1W)	0.2406(4)	0.9095(3)	0.8604(2)	0.017(1)
N(1)	− 0.0167(4)	0.2522(3)	0.9271(2)	0.012(1)
N(2)	0.0732(4)	0.5777(3)	0.8179(2)	0.015(1)
N(3)	− 0.2671(4)	1.3117(3)	0.5589(2)	0.014(1)
N(4)	− 0.0145(4)	1.0176(3)	0.6619(2)	0.015(1)
C(1)	− 0.1434(5)	0.3443(4)	0.8592(2)	0.015(1)
C(2)	− 0.0971(5)	0.5062(4)	0.8043(2)	0.017(1)
C(3)	0.1960(5)	0.4865(4)	0.8892(2)	0.015(1)
C(4)	0.1518(5)	0.3237(4)	0.9427(2)	0.013(1)
C(5)	0.2905(5)	0.2133(4)	1.0205(2)	0.015(1)
C(6)	− 0.0595(5)	1.2586(4)	0.5259(2)	0.016(1)
C(7)	0.0665(6)	1.1096(4)	0.5772(2)	0.017(1)
C(8)	− 0.2238(6)	1.0748(4)	0.6958(2)	0.016(1)
C(9)	− 0.3500(5)	1.2207(4)	0.6440(2)	0.014(1)
C(10)	− 0.5893(6)	1.2828(4)	0.6740(2)	0.016(1)

[a] *U*(eq) is defined as one-third of the trace of the orthogonalized U_{ij} tensor.

868, 795, and 743 cm^{-1} are due to the coordinated pyrazine moiety (7, 15).

Thermal analyses of the four compounds were performed in the temperature range 30–600°C. It is observed that compounds **1** and **3** start to decompose at ca. 50°C, a much lower temperature than that observed for **2** and **4** (ca. 180°C). Between 50 and 220°C, the weight losses for **1** and **3** are 4.8 and 3.4%, respectively, corresponding to the release of one water molecule per formula unit (Calc. 4.2% for **1**, 3.8% for **3**). The weight losses for **2** and **4** in the range 180–242°C are 4.1 and 3.9%, respectively, also agree well with the removal of one water molecule. Above 250°C, the behaviors of all four compounds are similar and are due to the decomposition of the organic ligand and the collapse of the crystal lattice. The difference in the first-step decomposition temperatures of the α-phase (**1** and **3**) and the β-phase (**2** and **4**) suggests different coordination modes of water molecules in the two phases. Such different coordination modes are confirmed by the single crystal structure determinations.

Crystal Structures of **1** *and* **3**

Compounds **1** and **3** both exhibit a two-dimensional structure built up from mixed valence chains of $Cu^{I}Cu^{II}(2\text{-pzc})_2(H_2O)$ linked by halide anions. Figure 1 shows a fragment of the layer in compound **1** with the atomic labeling scheme. Two kinds of copper ions are crystallographically distinguishable. The Cu(1) atom is divalent and has a square pyramidal coordination geometry, whereas the Cu(2) atom

TABLE 6
Selected Bond Lengths (Å) and Angles (°) for 1

Cu(1)–O(1)	1.943(3)	Cu(1)–O(3)	1.956(3)
Cu(1)–N(3)	2.002(4)	Cu(1)–N(1)	2.001(4)
Cu(1)–O(1W)	2.207(4)	Cu(2)–N(4)[a]	1.984(4)
Cu(2)–N(2)	1.988(4)	Cu(2)–Cl(1)	2.376(1)
Cu(2)–Cl(1)[b]	2.564(2)		
O(1)–Cu(1)–O(3)	171.5(2)	O(1)–Cu(1)–N(1)	83.0(2)
O(1)–Cu(1)–N(3)	97.8(2)	O(3)–Cu(1)–N(3)	82.8(2)
O(3)–Cu(1)–N(1)	95.8(2)	N(3)–Cu(1)–N(1)	176.3(2)
O(1)–Cu(1)–O(1W)	95.1(2)	O(3)–Cu(1)–O(1W)	93.3(2)
N(3)–Cu(1)–O(1W)	91.5(2)	N(1)–Cu(1)–O(1W)	92.1(2)
N(4)[a]–Cu(2)–N(2)	142.9(2)	N(4)[a]–Cu(2)–Cl(1)	98.5(1)
N(2)–Cu(2)–Cl(1)	100.8(1)	N(4)[a]–Cu(2)–Cl(1)[b]	97.8(1)
N(2)–Cu(2)–Cl(1)[b]	98.8(1)	Cl(1)–Cu(2)–Cl(1)[b]	121.1(1)
Cu(2)–Cl(1)–Cu(2)[c]	125.4(1)	C(10)–O(3)–Cu(1)	116.0(3)
C(5)–O(1)–Cu(1)	115.8(3)	C(1)–N(1)–Cu(1)	130.4(3)
C(4)–N(1)–Cu(1)	111.3(3)	C(2)–N(2)–Cu(2)	119.8(3)
C(3)–N(2)–Cu(2)	122.0(3)	C(7)–N(4)–Cu(2)[d]	121.8(3)
C(8)–N(4)–Cu(2)[d]	120.0(3)	C(6)–N(3)–Cu(1)	131.0(3)
C(9)–N(3)–Cu(1)	111.8(3)		

Note. Symmetry transformations used to generate equivalent atoms: [a] $x, -y+1/2, z-1/2$; [b] $-x+3/2, y-1/2, z$; [c] $-x+3/2, y+1/2, z$; [d] $x, -y+1/2, z+1/2$

TABLE 7
Selected Bond Lengths (Å) and Angles (°) for 2

Cu(1)–O(1)	1.963(4) 2×	Cu(1)–N(1)	2.025(5)2×
Cu(2)–N(2)	1.995(5)	Cu(2)–N(4)	2.034(5)
Cu(2)–Cl	2.322(2)	Cu(2)–O(1W)	2.326(5)
Cu(3)–O(3)	1.930(4) 2×	Cu(3)–N(3)	1.996(5) 2×
Cu(1)–O(1w)[a]	2.460(5) 2×	Cu(3)–Cl[b]	2.879(2) 2×
O(1)–Cu(1)–O(1)[c]	180.0	N(1)–Cu(1)–N(1)[c]	180.0
O(1)–Cu(1)–N(1)	83.7(2) 2×	O(1)[c]–Cu(1)–N(1)	96.3(2) 2×
N(2)–Cu(2)–N(4)	128.2(2)	N(2)–Cu(2)–Cl	121.0(2)
N(4)–Cu(2)–Cl	105.0(2)	N(2)–Cu(2)–O(1W)	92.5(2)
N(4)–Cu(2)–O(1W)	97.5(2)	Cl–Cu(2)–O(1W)	105.16(13)
O(3)–Cu(3)–O(3)[d]	180.0	N(3)–Cu(3)–N(3)[d]	180.0
O(3)–Cu(3)–N(3)	84.1(2) 2×	O(3)–Cu(3)–N(3)[d]	95.9(2) 2×
C(5)–O(1)–Cu(1)	114.0(4)	C(10)–O(3)–Cu(3)	114.3(4)
C(1)–N(1)–Cu(1)	131.2(4)	C(4)–N(1)–Cu(1)	109.2(4)
C(2)–N(2)–Cu(2)	125.0(5)	C(3)–N(2)–Cu(2)	118.6(4)
C(6)–N(3)–Cu(3)	132.0(4)	C(9)–N(3)–Cu(3)	110.0(4)
C(7)–N(4)–Cu(2)	121.4(4)	C(8)–N(4)–Cu(2)	121.5(4)

Note. Symmetry transformations used to generate equivalent atoms: [a] $x, y-1, z$; [b] $x-1, y+1, z$; [c] $-x, -y, -z+2$; [d] $-x-1, -y+3, -z+1$.

is monovalent with a tetrahedral coordination environment. The basal plane of the $\{Cu(1)N_2O_3\}$ square pyramid is defined by N(1), N(3), O(1), and O(3) atoms from two 2-pzc ligands, with the largest deviation of 0.0409 Å at the N(1) atom. The Cu(1) atom deviates from this plane by 0.1022 Å. The apical position is filled by O(1w) of the water molecule. The Cu(1)–O [1.943(3), 1.956(3) Å] and Cu(1)–N [2.001(4), 2.002(4) Å] distances are in agreement with those in

TABLE 8
Selected Bond Lengths (Å) and Angles (°) for 3

Cu(1)–O(3)	1.945(2)	Cu(1)–O(1)	1.949(2)
Cu(1)–N(3)	2.008(2)	Cu(1)–N(1)	2.009(2)
Cu(1)–O(1W)	2.301(2)	Cu(2)–N(2)	1.988(2)
Cu(2)–N(4)[a]	1.997(2)	Cu(2)–Br	2.5716(4)
Cu(2)–Br[b]	2.7592(4)		
O(3)–Cu(1)–O(1)	178.12(8)	O(3)–Cu(1)–N(3)	82.90(7)
O(1)–Cu(1)–N(3)	96.76(7)	O(3)–Cu(1)–N(1)	97.61(7)
O(1)–Cu(1)–N(1)	82.87(7)	N(3)–Cu(1)–N(1)	175.50(8)
O(3)–Cu(1)–O(1W)	92.03(8)	O(1)–Cu(1)–O(1W)	89.80(8)
N(3)–Cu(1)–O(1W)	87.31(8)	N(1)–Cu(1)–O(1W)	88.20(8)
N(2)–Cu(2)–N(4)[a]	147.20(9)	N(2)–Cu(2)–Br	98.10(6)
N(4)[a]–Cu(2)–Br	97.56(6)	N(2)–Cu(2)–Br[b]	97.53(6)
N(4)[a]–Cu(2)–Br[b]	98.03(6)	Br–Cu(2)–Br[b]	122.519(14)
Cu(2)–Br–Cu(2)[c]	110.142(12)	C(1)–N(1)–Cu(1)	130.9(2)
C(4)–N(1)–Cu(1)	110.9(2)	C(2)–N(2)–Cu(2)	122.1(2)
C(3)–N(2)–Cu(2)	121.2(2)	C(6)–N(3)–Cu(1)	130.5(2)
C(9)–N(3)–Cu(1)	111.3(2)	C(5)–O(1)–Cu(1)	115.7(2)
C(10)–O(3)–Cu(1)	116.0(2)		

Note. Symmetry transformations used to generate equivalent atoms: [a] $x, -y+1/2, z+1/2$; [b] $-x+3/2, y-1/2, z$; [c] $-x+3/2, y+1/2, z$; [d] $x, -y+1/2, z-1/2$

TABLE 9
Selected Bond Lengths (Å) and Angles (°) for 4

Cu(1)–O(1)	1.966(2) 2×	Cu(1)–N(1)	2.005(2) 2×
Cu(1)–O(1W)[a]	2.439(2) 2×	Cu(2)–N(2)	1.998(3)
Cu(2)–N(4)	2.020(3)	Cu(2)–O(1W)	2.293(2)
Cu(2)–Br	2.4690(5)	Cu(3)–O(3)	1.937(2) 2×
Cu(3)–N(3)	1.996(3) 2×	Cu(3)–Br[b]	3.016(1) 2×
O(1)[c]–Cu(1)–O(1)	180.0	N(1)–Cu(1)–N(1)[c]	180.0
O(1)[c]–Cu(1)–N(1)	96.75(10) 2×	O(1)–Cu(1)–N(1)	83.25(10)
O(1)[c]–Cu(1)–O(1W)[a]	87.91(9) 2x	O(1)–Cu(1)–O(1W)[a]	92.09(9) 2×
N(1)–Cu(1)–O(1W)[a]	87.35(9) 2×	N(1)–Cu(1)–O(1W)[d]	92.65(9) 2×
O(1W)[a]–Cu(1)–O(1W)[d]	180.0	N(2)–Cu(2)–N(4)	130.60(11)
N(2)–Cu(2)–O(1W)	94.15(10)	N(4)–Cu(2)–O(1W)	99.75(10)
N(2)–Cu(2)–Br	116.88(8)	N(4)–Cu(2)–Br	105.21(8)
O(1W)–Cu(2)–Br	104.12(6)	O(3)[e]–Cu(3)–O(3)	180.0
O(3)[e]–Cu(3)–N(3)	96.10(10) 2×	O(3)–Cu(3)–N(3)	83.90(10) 2×
N(3)–Cu(3)–N(3)[e]	180.0	Cu(2)–O(1W)–Cu(1)[f]	130.31(11)
C(5)–O(1)–Cu(1)	115.0(2)	C(10)–O(3)–Cu(3)	114.4(2)
C(1)–N(1)–Cu(1)	131.0(2)	C(4)–N(1)–Cu(1)	110.4(2)
C(2)–N(2)–Cu(2)	123.8(2)	C(3)–N(2)–Cu(2)	119.2(2)
C(6)–N(3)–Cu(3)	131.4(2)	C(9)–N(3)–Cu(3)	110.2(2)
C(7)–N(4)–Cu(2)	121.4(2)	C(8)–N(4)–Cu(2)	121.3(2)

Note. Symmetry transformations used to generate equivalent atoms: [a] $x, y-1, z$; [b] $x-1, y+1, z$; [c] $-x, -y, -z+2$; [d] $-x, -y+1, -z+2$; [e] $-x-1, -y+3, -z+1$; [f] $x, y+1, z$

$[KCu_2(2\text{-pzc})(N_3)_4]_n$ [Cu–O 1.954(5), Cu–N 2.010(4)–2.022(4) Å] (7), $Cu(2\text{-pzc})_2$ [Cu–O 1.93(1), Cu–N 1.98(1) Å], and $Cu(2\text{-pzc})_2(H_2O)_2$ [Cu–O 1.98(1), Cu–N 2.00(1) Å] (16). The Cu(1)–O(1w) distance [2.207(4) Å] is slightly longer. The $\{Cu(1)(2\text{-pzc})_2(H_2O)\}$ units in **1** are linked by cuprous ions Cu(2) through bonding to the remaining nitrogen atoms N(2) and N(4) of the pyrazine moieties, forming infinite chains approximately along the *c*-axis. The basal planes of the $\{Cu(1)N_2O_3\}$ square pyramids within the chain are nearly coplanar, with the interplane angle being 0.8°. The $\{Cu(2)N_2Cl_2\}$ tetrahedra, on the other hand, are corner-shared by Cl^- anions forming an infinite chain along [100] direction. Consequently, a two-dimensional layer structure is constructed by cross-linking of the two types of chains, as shown in Fig. 2.

Weak hydrogen bonds are found within the layer and between the layers. The two shortest contacts are $O(1w)\cdots O(1)^{i}$ [2.723(3) Å] and $O(1w)\cdots O(3)^{ii}$ [2.725(3) Å] (symmetry code: i, $1.5-x, y-0.5, z$; ii, $1.5-x, y+0.5, z$).

The structure of **3** is very similar to that of **1**. Within the layer, there exist chains of $Cu^{I}Cu^{II}(2\text{-pzc})_2(H_2O)$ interlinked by the corner-sharing $\{Cu(2)N_2Br_2\}$ tetrahedra. The bond lengths and angles are comparable to those in **1** (Tables 6 and 8). The packing of these layers in **3**, however, is slightly different from that in **1**. In the former case, all the pyrazine rings are stacked above each other along the *a*-axis (Fig. 3), whereas in the latter case, the stacking of the pyrazine rings in adjacent sheets are shifted. This subtle difference could be caused by weak interactions between Br^- and the Cu(1)

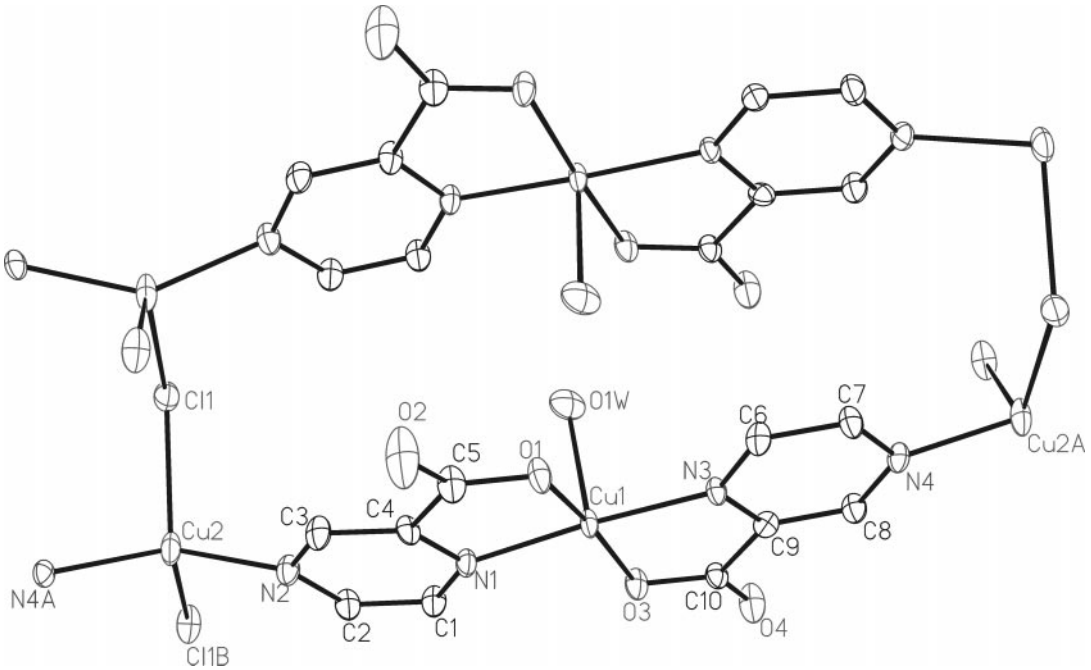

FIG. 1. A fragment of the layer in compound **1** with atomic labeling scheme (50%).

atoms in the neighboring layers in **3**. The shortest Cu(1) ··· Br distance between the layers is 3.167 Å for **3**. For **1**, the closest interlayer contact to the Cu(1) atom is from the O(4) atom [Cu(1) ··· $O(4)^{iii}$ = 3.163 Å, symmetry code: iii, $1 - x$, $0.5 + y$, $1.5 - z$].

Crystal Structures of **2** *and* **4**

The two compounds are isostructural. They are isomers of **1** and **3**, respectively. Taking **4** as an example, Fig. 4 shows a fragment of the infinite chain of $Cu^{I}Cu^{II}(2\text{-pzc})_2$ similar to that in **1** and **3**. Within the chain, three copper atoms are crystallographically distinguishable. Both the Cu(1) and the Cu(3) atoms are divalent and have octahedral geometries. The axial positions are occupied by two water molecules for Cu(1) and by two Br anions for Cu(3). The basal planes of the Cu(1) and Cu(3) octahedra are not coplanar. The interplane angle is 56.2°, which differs significantly from that in **1** (0.8°) or **3** (1.6°). The monovalent Cu(2) has a tetrahedral coordination environment. Each

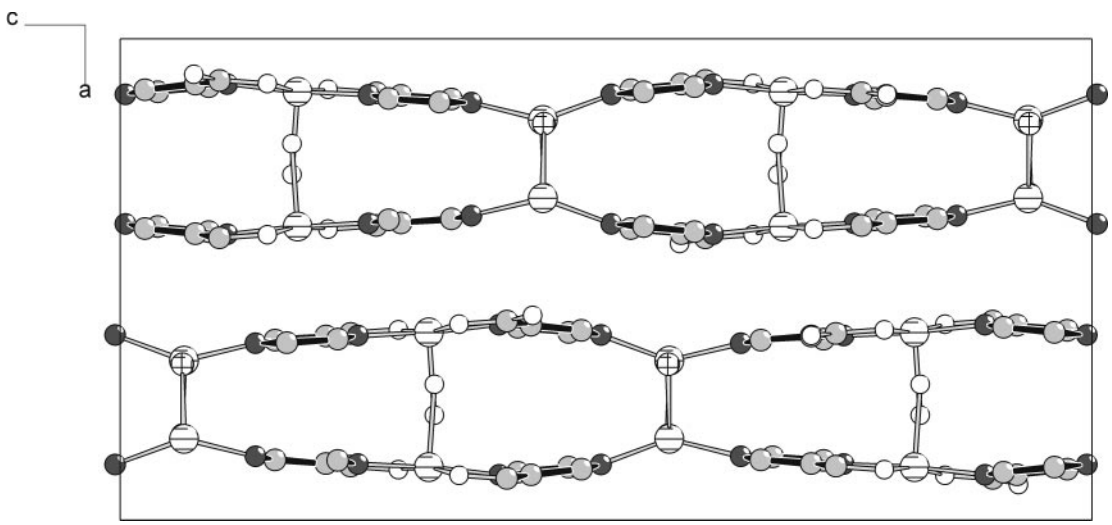

FIG. 2. Packing diagram of the structure of **1** along [010] direction. All H atoms are omitted for clarity.

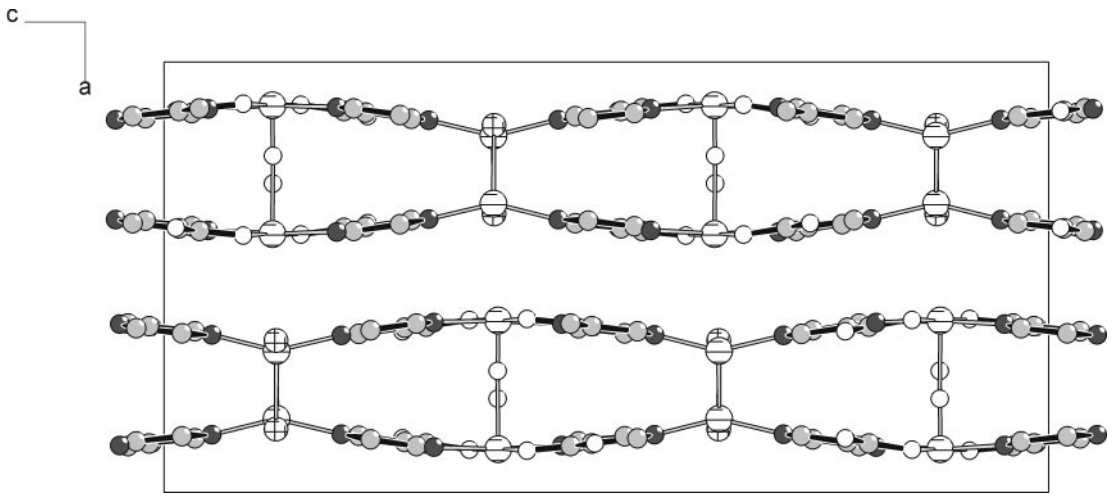

FIG. 3. Packing diagram of the structure of **3** along [010] direction. All H atoms are omitted for clarity.

$\{Cu^{I}(2)N_2BrO(1w)\}$ tetrahedron shares the Br atom with a $\{Cu^{II}(3)N_2O_2Br_2\}$ octahedron and the O(1w) atom with a $\{Cu^{II}(1)N_2O_2O(1w)_2\}$ octahedron, forming alternatively arranged octahedra–tetrahedra chains (Fig. 5). A three-dimensional structure is therefore constructed by linking the Cu^{I} and Cu^{II} through 2-pzc, O(1w) and Br bridges.

The bond lengths and angles around the copper ions are comparable to those in **3**, although the Cu(1)–O(1w) [2.439 Å] and Cu(3)–Br [3.016 Å] distances are slightly longer. Relatively long Cu–OH_2 and Cu–Br distances have been observed in other complexes such as $[Cu_2(OH)_2(H_2O)(dpyam)_2]Cl_2 \cdot 2H_2O$ (dpyam = 2,2′-dipyridylamine) [Cu–OH_2 2.414(6) Å] (17), $Cu_2L(OH)(ClO_4)_3 \cdot 2H_2O$ (L = 20-membered macrocyclic tetraimine) [Cu–OH_2 2.519(12) Å] (18), $\{Cu(TMSO)_4\}[Cu_2Br_6]$, and $[C_8H_6N_4Br_4Cu_2]_n$ [Cu–Br 3.018–3.063 Å] (19, 20).

UV–Vis Spectroscopic and Magnetic Properties

The solid UV–vis spectra in the 350 to 1400-nm region show that the absorptions of compounds **1**–**4** cover almost the whole visible region (Fig. 6), which is in agreement with their black or dark red colors. The result indicates that charge transfer from Cu(I) to Cu(II) could occur in these compounds. It is noted that the spectra of **2** and **4** are very similar to each other. The difference between the spectra of

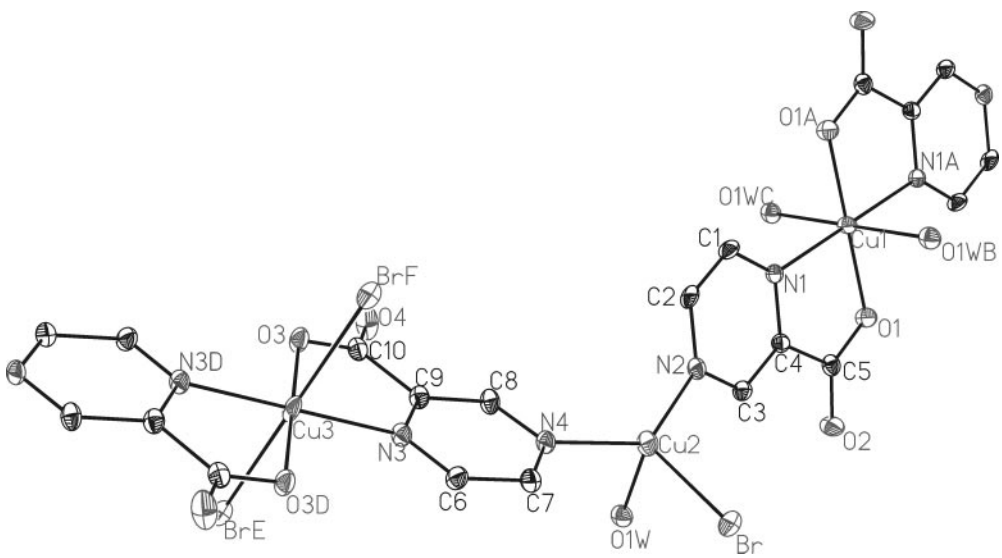

FIG. 4. A fragment of the $Cu^{I}Cu^{II}(2\text{-pzc})_2$ chain in compound **4** with atomic labeling scheme (50%).

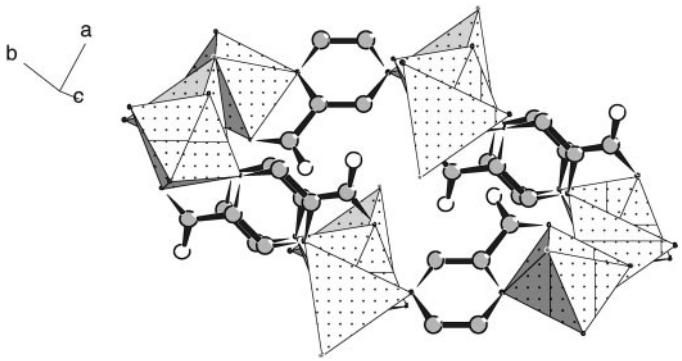

FIG. 5. Polyhedral representation of the structure of **4**. All the H atoms are omitted for clarity.

1 and **3** may be related to their different structures. Significant Cu–Br interlayer interactions are present in **3** because of the layer stacking.

The temperature-dependent magnetic susceptibilities for **1** and **2** were measured in the range 300 to 2 K. At 300 K, the magnetic moment (μ_{eff}) per copper(II) atom, determined from the equation $\mu_{\text{eff}} = 2.828(\chi_{\text{m}}T)^{1/2}$, is 1.72 μ_{B} for both compounds which is close to the value expected for an isolated system of $S = 1/2$ ($\mu_{\text{eff}} = 1.73\ \mu_{\text{B}}$). Considering the structures, the closest Cu(II)$\cdots$Cu(II) distances in **1** are 13.050 Å within $[Cu^{I}Cu^{II}(C_5H_3N_2O_2)_2(H_2O)]$ chain and 5.290 Å between the chains, whereas that in **2** is 7.725 Å. Therefore, the interactions between the magnetic centers in both compounds are anticipated to be very weak. The data were analyzed by Curie–Weiss law, based on the equation

$$\chi_{\text{m}} = C/(T - \theta) + N_{\alpha},$$

where C is Curie constant, θ is Weiss constant, and N_{α} accounts for the diamagnetic contribution. An excellent fit was obtained for **1** with the parameters $C = 0.417\ \text{cm}^3\ \text{K mol}^{-1}$, $\theta = -0.15$ K, and $N_{\alpha} = -0.000182\ \text{cm}^3\ \text{mol}^{-1}$. The agreement factor R defined as $\sum_i[(\chi_{\text{m}})_{\text{obs}}(i) - (\chi_{\text{m}})_{\text{calc}}(i)]^2/\sum_i[(\chi_{\text{m}})_{\text{obs}}(i)]^2$ is 2.85×10^{-5}. For compound **2**, a good fit also resulted: $C = 0.384\ \text{cm}^3\ \text{K mol}^{-1}$, $\theta = -0.39$ K, $N_{\alpha} = -0.000127\ \text{cm}^3\ \text{mol}^{-1}$, $R = 1.76 \times 10^{-6}$. The negative Weiss constants (θ) indicate only very weak antiferromagnetic exchange coupling in both cases.

In summary, under mild hydrothermal reaction conditions, four new mixed valence copper compounds with the formula α-, β-$[Cu_2X(C_5H_3N_2O_2)_2(H_2O)]$ (X = Cl, Br) have been prepared and their structures determined. It is interesting to note that in **1** and **3** (α-phase) the Cu^{I} and Cu^{II} are purely bridged by the 2-pzc ligand, whereas in **2** and **4** (β-phase) the halide ions and water molecules also serve as bridging ligands. The existence of the bridging water molecule in the latter cases explains their higher decomposition temperatures during the thermal analyses. Additionally, the 2D structure of the α-phase and the 3D structure of the β-phase, although significantly different, are closely related to each other. Both are based on the fundamental building unit $\{Cu^{I}Cu^{II}(2\text{-pzc})_2\}$. In the α-phase, the$\{Cu^{I}N_2X_2\}$ tetrahedra are corner-shared with each other through halide anions. In the β-phase, each $\{Cu^{I}N_2XO(1w)\}$ tetrahedron shares the X corner with a $\{Cu^{II}(3)N_2O_2X_2\}$ octahedron and the O(1w) corner with a $\{Cu^{II}(1)N_2O_2O(1w)_2\}$ octahedron. Finally, different bridging ligands in the β-phase may provide versatile pathways to transfer electron densities between Cu^{I} and Cu^{II} which could be of interest in understanding the electron-transfer mechanism in such systems.

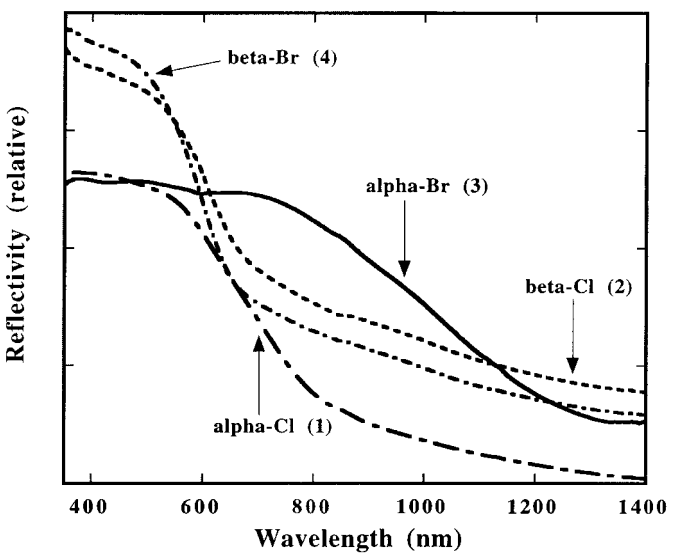

FIG. 6. UV–vis spectra for **1**–**4**.

ACKNOWLEDGMENTS

We thank the National Science Foundation (DMR-9805881) and the R. A. Welch Foundation for financial support. This work made use of MRSEC/TCSUH Shared Experimental Facilities supported by the National Science Foundation under Award DMR-9632667 and the Texas Center for Superconductivity at the University of Houston. We also thank Varian, Inc., for providing the UV–vis spectra and Mr. Yongsheng Wang for the magnetic measurements.

REFERENCES

1. K. D. Karlin and J. Zubieta (Eds.), "Copper Coordination Chemistry: Biological and Inorganic Perspectives," Adenine Press, New York, 1985.
2. K. D. Karlin and J. Zubieta (Eds.), "Biological and Inorganic Copper Chemistry," Adenine Press, New York, 1986.
3. P. A. Cox, "Transition Metal Oxides: An Introduction to Their Electronic Structure and Properties," Clarendron Press, Oxford, 1995.
4. M. B. Robin and P. Day, *Adv. Inorg. Radiochem.* **10,** 247 (1967).
5. S. R. Breeze and S. Wang, *Inorg. Chem.* **35,** 3404 (1996).
6. T. J. Meyer, *Acc. Chem. Res.* **11,** 94 (1978).

7. M. A. S. Goher, N. A. Al-Salem, F. A. Mautner, and K. O. Klepp, *Polyhedron* **16,** 825 (1997).
8. J. M. Moreno, J. Suarez-Varela, E. Colacio, J. C. Avila-Rosón, M. A. Hidalgo, and D. Martin-Ramos, *Can. J. Chem.* **73,** 1591 (1995).
9. R. Kuhlman, G. L. Schimek, and J. W. Kolis, *Polyhedron* **18,** 1379 (1999).
10. Unit cell constants for the yellow compound: triclinic, space group $P1$, $a = 3.945(8)$, $b = 6.999(14)$, $c = 7.845(15)$ Å, $\alpha = 107.67(3)$, $\beta = 100.14(3)$, $\gamma = 94.55(3)^\circ$, $V = 201.1(26)$ Å ^{3}.
11. S. Kawata, S. Kitagawa, H. Kumagai, S. Iwabuchi, and M. Katada, *Inorg. Chim. Acta* **267,** 143 (1998).
12. "SAINT, Program for Data Extraction and Reduction," Siemens Analytical X-ray Instruments, Madison, WI 53719, 1994–1996.
13. G. M. Sheldrick, "SADABS, Program for Siemens Area Detector Absorption Corrections," University of Göttingen, Germany, 1997.
14. G. M. Sheldrick, "SHELXTL, Program for Refinement of Crystal Structures," Siemens Analytical X-ray Instruments, Madison, WI 53719, 1994.
15. K. Nakamoto, "Infrared and Raman Spectra of Inorganic and Coordination Compounds," Wiley, New York, 1997.
16. C. L. Klein, R. J. Majeste, L. M. Trefonas, and C. J. O'Connor, *Inorg. Chem.* **21,** 1891 (1982).
17. L.-P. Wu, M. E. Keniry, and B. Hathaway, *Acta Crystallogr.* **48C,** 35 (1992).
18. M. G. B. Drew, J. Nelson, F. Esho, V. McKee, and S. M. Nelson, *J. Chem. Soc., Dalton Trans.* 1837 (1982).
19. C. P. Landee, A. Djili, D. F. Mudgett, M. Newhall, H. Place, B. Scott, and R. D. Willett, *Inorg. Chem.* **27,** 620 (1988)
20. M. Julve, G. De Munno, G. Bruno, and M. Verdaguer, *Inorg. Chem.* **27,** 3160 (1988).